

Low background detector with enriched $^{116}\text{CdWO}_4$ crystal scintillators to search for double β decay of ^{116}Cd

A.S. Barabash^a, P. Belli^b, R. Bernabei^{b,c,*}, R.S. Boiko^d, F. Cappella^{e,f},
V. Caracciolo^{g,h}, D.M. Chernyak^d, R. Cerulli^g, F.A. Danevich^d, M.L. Di Vacri^g,
A.E. Dossovitskiyⁱ, E.N. Galashov^j, A. Incicchitti^{e,f}, V.V. Kobychiev^d,
S.I. Konovalov^a, G.P. Kovtun^k, V.M. Kudovbenko^d, M. Laubenstein^g, A.L. Mikhlinⁱ,
S. Nisi^g, D.V. Poda^{g,d}, R.B. Podvivanuk^d, O.G. Polischuk^d, A.P. Shcherban^k,
V.N. Shlegel^j, D.A. Solopikhin^k, Yu.G. Stenin^j, V.I. Tretyak^d, V.I. Umatov^a,
Ya.V. Vasiliev^j, V.D. Virich^k

^a*Institute of Theoretical and Experimental Physics, 117259 Moscow, Russia*

^b*INFN sezione Roma "Tor Vergata", I-00133 Rome, Italy*

^c*Dipartimento di Fisica, Università di Roma "Tor Vergata", I-00133, Rome, Italy*

^d*Institute for Nuclear Research, MSP 03680 Kyiv, Ukraine*

^e*INFN sezione Roma "La Sapienza", I-00185 Rome, Italy*

^f*Dipartimento di Fisica, Università di Roma "La Sapienza", I-00185 Rome, Italy*

^g*INFN, Laboratori Nazionali del Gran Sasso, I-67100 Assergi (AQ), Italy*

^h*Dipartimento di Fisica, Università dell'Aquila, I-67100 L'Aquila, Italy*

ⁱ*Joint Stock Company NeoChem, 117647 Moscow, Russia*

^j*Nikolaev Institute of Inorganic Chemistry, 630090 Novosibirsk, Russia*

^k*National Science Center "Kharkiv Institute of Physics and Technology", 61108 Kharkiv, Ukraine*

E-mail: rita.bernabei@roma2.infn.it

ABSTRACT: A cadmium tungstate crystal boule enriched in ^{116}Cd to 82% with mass of 1868 g was grown by the low-thermal-gradient Czochralski technique. The isotopic composition of cadmium and the trace contamination of the crystal were estimated by High Resolution Inductively Coupled Plasma Mass-Spectrometry. The crystal scintillators produced from the boule were subjected to characterization that included measurements of transmittance and energy resolution. A low background scintillation detector with two $^{116}\text{CdWO}_4$ crystal scintillators (586 g and 589 g) was developed. The detector was running over 1727 h deep underground at the Gran Sasso National Laboratories of the INFN (Italy), which allowed to estimate the radioactive contamination of the enriched crystal scintillators. The radiopurity of a third $^{116}\text{CdWO}_4$ sample (326 g) was tested with the help of ultra-low background high purity germanium γ detector. Monte Carlo simulations of double β processes in ^{116}Cd were used to estimate the sensitivity of an experiment to search for double β decay of ^{116}Cd .

KEYWORDS: Double beta decay; CdWO₄ crystal scintillator; Enriched isotope ¹¹⁶Cd; Low counting experiment; Radiopurity.

*Corresponding author.

Contents

1. Introduction	1
2. Development of $^{116}\text{CdWO}_4$ crystal scintillators	2
2.1 Contamination of enriched ^{116}Cd	2
2.2 Recovery of enriched cadmium ^{116}Cd from cadmium tungstate crystalline residue	3
2.3 Purification of enriched cadmium by vacuum distillation and filtering	4
2.4 Synthesis of $^{116}\text{CdWO}_4$ compound	4
2.5 Growth of $^{116}\text{CdWO}_4$ crystal and production of scintillation elements	5
3. Characterisation of $^{116}\text{CdWO}_4$ crystal scintillators	5
3.1 Isotopic composition of cadmium in the $^{116}\text{CdWO}_4$ crystal	5
3.2 Light transmission	6
3.3 Energy resolution	7
4. Low background measurements, results and discussion	8
4.1 Measurements with ultra-low background HPGe γ ray spectrometry	8
4.2 Low background detector system with $^{116}\text{CdWO}_4$ crystal scintillators	8
4.3 Data analysis	11
4.3.1 Pulse-shape discrimination	12
4.3.2 Time-amplitude analysis of ^{228}Th and ^{227}Ac contaminations	13
4.3.3 Selection of Bi–Po events	14
4.4 Background in the region of $Q_{\beta\beta}$ of ^{116}Cd	16
5. Monte Carlo simulation of double β decay of ^{116}Cd, estimations of experimental sensitivity	18
6. Conclusions	20
7. Acknowledgements	21

1. Introduction

The neutrinoless mode of the double beta decay ($0\nu 2\beta$) is a powerful tool to investigate properties of neutrino and weak interactions. Even negative results of double β decay experiments provide important information on the absolute scale and hierarchy of the Majorana neutrino mass, lepton number conservation, right-handed admixtures in weak interaction, existence of majorons, and other effects beyond the Standard Model [1].

The cadmium 116 is one of the most prospective isotopes to search for $0\nu 2\beta$ decay thanks to the high energy of the decay $Q_{\beta\beta} = 2809 \pm 4$ keV [2], the relatively large isotopic abundance 7.49 ± 0.18 % [3], the promising theoretical predictions [4, 5, 6] and the existence of cadmium tungstate (CdWO_4) crystal scintillators allowing to realize a calorimetric (“source = detector”) experiment.

The most sensitive 2β experiment to search for double beta decay of ^{116}Cd was performed in the Solotvina Underground Laboratory with the help of cadmium tungstate crystal scintillators enriched in ^{116}Cd ($^{116}\text{CdWO}_4$, see [7] and references therein). The two neutrino mode of 2β decay of ^{116}Cd was observed with the half-life $T_{1/2} = (2.9_{-0.3}^{+0.4}) \times 10^{19}$ yr, and the half-life limit on $0\nu 2\beta$ decay of ^{116}Cd was set as $T_{1/2} \geq 1.7 \times 10^{23}$ yr at 90% C.L. It corresponds to an upper bound on the effective Majorana neutrino mass $\langle m_\nu \rangle \leq 1.7$ eV [7]. Searches for double β processes in ^{106}Cd , ^{108}Cd and ^{114}Cd were realized by using low background CdWO_4 crystal scintillators produced from cadmium of the natural composition [8, 9]. Recently, a cadmium tungstate crystal scintillator enriched in ^{106}Cd was developed [10], and an experiment to search for double beta processes in ^{106}Cd with the help of this detector is in progress in the Gran Sasso Underground Laboratories [11]. In addition, cadmium tungstate crystal scintillators were also successfully applied to study the fourth-forbidden β decay of ^{113}Cd [12, 13] and to detect, for the first time, the α decay of ^{180}W with the half-life $T_{1/2} = (1.1_{-0.5}^{+0.9}) \times 10^{18}$ yr [14].

High sensitivity double β experiments require detectors with maximal concentration of the studied isotope, high detection efficiency to double β processes, low (ideally zero) level of radioactive contamination and ability of particle discrimination to further reduce the background, good energy resolution, large mass, and stability of operation over long (several years) time.

In the next Section we describe the development of large volume cadmium tungstate crystal enriched in ^{116}Cd . The characterization of $^{116}\text{CdWO}_4$ crystal scintillators produced from the crystal is presented in Section 3. The low background detector with the enriched scintillators is described in Section 4. The data of low background measurements, both in scintillation mode and with the help of ultra-low background high purity germanium (HPGe) γ ray spectrometry, were analyzed to estimate radioactive contamination of the crystal scintillators. Finally we have simulated the detector response to the double β decay processes in ^{116}Cd and estimated the sensitivity to the neutrinoless double β decay of ^{116}Cd .

2. Development of $^{116}\text{CdWO}_4$ crystal scintillators

The production of crystal scintillators from enriched materials should satisfy some specific demands: minimal loss of expensive isotopically enriched material, high yield of crystals, prevention of radioactive contamination.

2.1 Contamination of enriched ^{116}Cd

To produce CdWO_4 crystals with good scintillation characteristics, it is necessary to control and minimize the contamination of the initial materials for the crystal growth at a level of 0.1 – 1 ppm for a range of elements. The most dangerous impurities which deteriorate optical and scintillation quality of cadmium tungstate crystals are transition metals (Ti, V, Cr, Mn, Fe, Co, Ni, Cu). Con-

centration of Ca, Al, Zn, Ag should also be under control. To obtain radiopure scintillators, one should avoid contamination by radioactive elements K, Th, U, Ra.

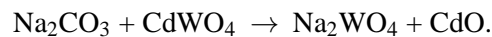
Samples of enriched cadmium of rather different purity grade were used in the present work. Some parts of the enriched material remained after the purification to produce $^{116}\text{CdWO}_4$ crystals for the Soltovina experiment, another part of ^{116}Cd oxide was extracted from the residual after the $^{116}\text{CdWO}_4$ crystal growth for the experiment [7] (see subsection 2.2). One portion of ^{116}Cd (316 g) was previously used in experiment to search for double beta decay of ^{116}Cd to the excited states of daughter nuclei [15].

The contamination of the enriched cadmium was measured with the help of High Resolution Inductively Coupled Plasma Mass Spectrometric analysis (Thermo Fisher Scientific ELEMENT2). Samples' dissolution was performed by microwave treatment according to the EPA 3052 method. Since the solids were not completely dissolved after the microwave digestion treatment, the supernatant of samples was analyzed by ICP MS in order to calculate the amount of dissolved sample. To enhance the sensitivity to Th and U, the sample solution was treated in an extraction chromatographic system in order to separate analytes from the matrix. This procedure allowed to reduce the dilution factor before analysis up to a value of 150 and to minimize the isobaric interferences between Th and WO_3 ions.

Potassium and iron were measured in High Resolution mode. Concentrations were calculated based on an external calibration method. We estimate the uncertainties of the measurements as about 15% of the given values. Thorium and uranium were measured in Medium Resolution mode while other elements were determined in Low Resolution High Sensitivity mode. A semiquantitative analysis was performed, that is a single standard solution containing some elements at a known concentration level (10 ppb of Li, Y, Ce, Tl) was used for calibration and quantification. The uncertainties when working in semiquantitative mode are about 25% of the given concentration value. The contribution of a blank procedure was estimated and subtracted from the samples. The analysis results are presented in Table 1.

2.2 Recovery of enriched cadmium ^{116}Cd from cadmium tungstate crystalline residue

A rest after $^{116}\text{CdWO}_4$ crystals growing for the Soltovina experiment was decomposed to extract enriched cadmium. Cadmium tungstate is not soluble in acids and alkalis. Molten sodium carbonate (Na_2CO_3 , TraceSelect, 99.9999%) was used as a solvent to decompose cadmium tungstate crystalline rest. A mixture of $^{116}\text{CdWO}_4$ and Na_2CO_3 in the mass proportion 1 : 1 was prepared, which corresponds to approximately 3.3 : 1 molar ratio. Then the mixture was heated in a platinum crucible at the temperature 950 °C over 4 hours. As a result the following reaction has occurred:



Sodium tungstate (Na_2WO_4) has the melting point of 696 °C. Therefore this compound was in the liquid phase at the temperature of the reaction, while cadmium oxide is insoluble both in the molten Na_2CO_3 and Na_2WO_4 salts and remained in the form of sediment. After the full decomposition of the cadmium tungstate the crucible was cooled down to room temperature. Solid Na_2CO_3 and Na_2WO_4 were dissolved in hot deionized water. Finally the precipitation of the enriched cadmium oxide was rinsed and dried.

Table 1. Contamination of initial enriched ^{116}Cd (the average value of several samples) and $^{116}\text{CdWO}_4$ crystal analyzed by ICP-MS analysis. The concentrations of impurities in the samples of ^{116}Cd oxide and the averaged contaminations of initial ^{116}Cd are normalized on the mass of cadmium.

Element	Concentration (ppm)		
	Samples of ^{116}Cd and ^{116}CdO	Averaged contamination of initial ^{116}Cd	$^{116}\text{CdWO}_4$ crystal
Mg	< 0.05 – 370	12	< 5
Al	< 0.5 – 58	8	< 15
K	< 5 – 17	< 10	5
Ca	< 6 – 37	19	< 150
Ti	< 0.1 – 7	1.5	0.8
V	< 0.005 – 0.16	0.01	< 0.15
Cr	< 0.05 – 26	2	< 0.8
Mn	< 0.1 – 3	0.7	< 0.3
Fe	< 0.07 – 150	14	3
Co	< 0.003 – 0.2	0.06	0.06
Ni	< 0.05 – 18	1.8	< 0.5
Cu	< 0.05 – 10	7	< 50
Zn	< 0.5 – 850	42	< 0.5
Ag	< 0.005 – 1	0.08	< 0.1
Ba	< 0.05 – 9	0.3	< 0.2
Th	< 0.001 – 0.003	< 0.02	< 0.00003
U	< 0.001 – 0.005	< 0.02	< 0.0004

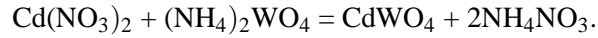
2.3 Purification of enriched cadmium by vacuum distillation and filtering

Most contaminated samples of enriched ^{116}Cd were purified by distillation through getters in the National Science Center “Kharkiv Institute of Physics and Technology” (Kharkiv, Ukraine) [16].

2.4 Synthesis of $^{116}\text{CdWO}_4$ compound

The powder to grow the $^{116}\text{CdWO}_4$ crystal was produced by the NeoChem company (Moscow, Russia). All the operations were carried out by using quartz or polypropylene lab-ware, materials with low level of radioactive contaminations. Reagents of high purity grade (concentration of any metal less than 0.01 ppm) were used. Water, acids and ammonia were additionally distilled by laminar evaporation in quartz installation. The high cost of the enriched ^{116}Cd limits the choice of the methods for its additional purification. Recrystallization methods, typically used for the cadmium salts purification, cannot be applied due to the low outcome of the final product (< 85%). Therefore, after dissolving the metallic cadmium in nitric acid, the purification was realized by coprecipitation on a collector. Additional recrystallization was performed to purify ammonium para-

tungstate used as tungsten source. Solutions of cadmium nitrate and ammonium para-tungstate were mixed and then heated to precipitate cadmium tungstate:



Then the $^{116}\text{CdWO}_4$ sediment was rinsed and filtered. Finally the $^{116}\text{CdWO}_4$ compound was dried and annealed.

2.5 Growth of $^{116}\text{CdWO}_4$ crystal and production of scintillation elements

The $^{116}\text{CdWO}_4$ crystal was grown by the low-thermal-gradient Czochralski technique [17, 18, 19] in a platinum crucible. Under low-thermal-gradient conditions the temperature of the melt was close to the melting point of cadmium tungsten crystal, which is ≈ 1270 °C. A crystal boule with mass of 1868 g (see Fig. 1, left) was grown from 2139 g of the initial $^{116}\text{CdWO}_4$ charge (87% of initial charge).

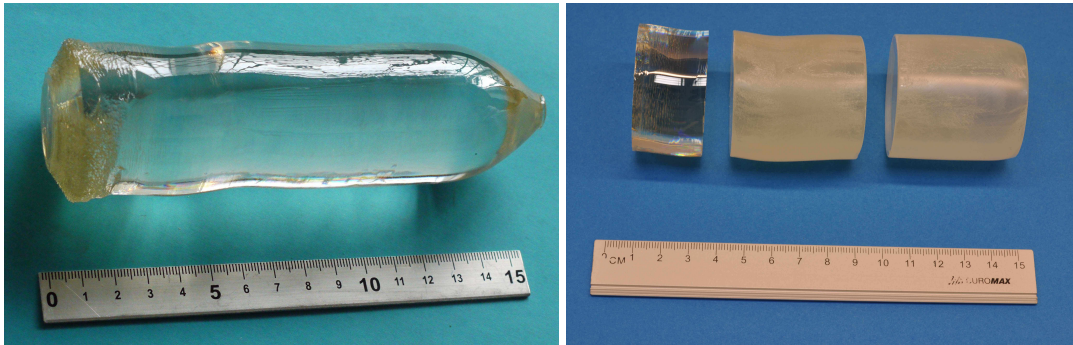


Figure 1. (Color online) Left: Boule of enriched $^{116}\text{CdWO}_4$ crystal. The conic part of the boule is the beginning of the crystal growth. Right: Crystal samples cut from the boule: $\approx \varnothing 45 \times 46.7$ mm, 586.2 g, No. 1 (right); $\approx \varnothing 45 \times 46.1$ mm, 589.3 g, No. 2 (middle); $\approx \varnothing 45.7 \times 25.1$ mm, 325.6 g, No. 3 (left).

Three near cylindrical shape crystal scintillators ($\varnothing 45 \times 46.7$ mm, 586.2 g, No. 1; $\varnothing 45 \times 46.1$ mm, 589.3 g, No. 2; $\varnothing 45.7 \times 25.1$ mm, 325.6 g, No. 3) have been cut from the crystal boule (see Fig. 1, right). The side surface of the crystals No.1 and 2 was diffused with the help of grinding paper to reach uniformity of scintillation light collection, which is important to improve energy resolution of the detector.

3. Characterisation of $^{116}\text{CdWO}_4$ crystal scintillators

3.1 Isotopic composition of cadmium in the $^{116}\text{CdWO}_4$ crystal

The isotopic composition of the cadmium in the enriched $^{116}\text{CdWO}_4$ crystal was measured with the help of the High Resolution Inductively Coupled Plasma Mass Spectrometric analysis. Results of the analysis are presented in Table 2. The absolute isotope abundance for ^{116}Cd is 82.2%, while β active ^{113}Cd has an absolute isotope abundance of 2.14%. The atomic weight of cadmium in the $^{116}\text{CdWO}_4$ crystal is 115.3 as compared to the table value of 112.411 ± 0.008 [20]. The atomic weight of $^{116}\text{CdWO}_4$ molecule is 363.1.

Table 2. The absolute isotopic composition of cadmium in the $^{116}\text{CdWO}_4$ crystal (%).

Atomic number	Enriched ^{116}Cd	Natural cadmium [3]
106	0.11 ± 0.01	1.25 ± 0.06
108	0.10 ± 0.01	0.89 ± 0.03
110	1.80 ± 0.05	12.49 ± 0.18
111	2.00 ± 0.05	12.80 ± 0.12
112	4.35 ± 0.04	24.13 ± 0.21
113	2.14 ± 0.06	12.22 ± 0.12
114	7.30 ± 0.06	28.73 ± 0.42
116	82.2 ± 0.1	7.49 ± 0.18

3.2 Light transmission

The transmittance of the $^{116}\text{CdWO}_4$ crystal scintillators was measured in the spectral range 330 – 700 nm using a PERKIN ELMER UV/VIS spectrometer Lambda 18. A thin (2.6 mm) sample of the $^{116}\text{CdWO}_4$ crystal was placed in the reference beam of the instrument to correct the reflection losses. The results of the optical transmission measurements for the $^{116}\text{CdWO}_4$ crystal No. 2 shown in Fig. 2 demonstrate that the material exhibits reasonable transmission properties in the relevant wavelength range 400 – 600 nm of the CdWO_4 emission spectrum.

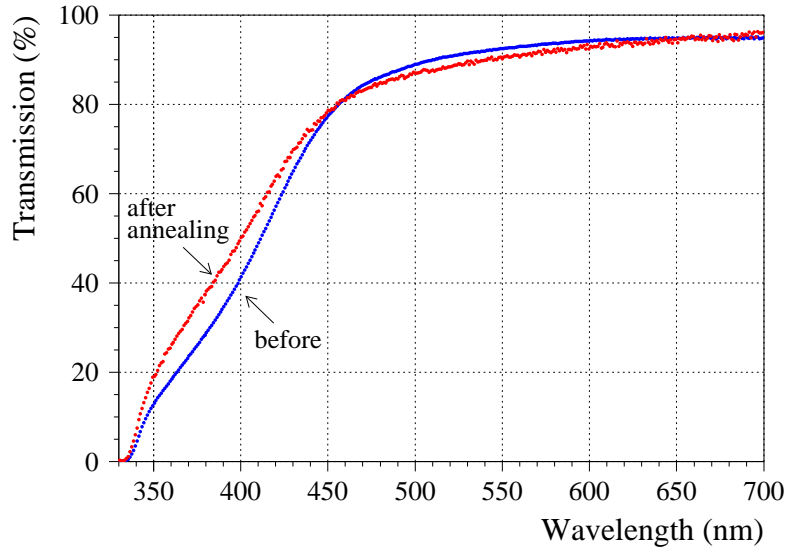


Figure 2. (Color online) The optical transmission curve of $^{116}\text{CdWO}_4$ crystal No. 2 before and after annealing measured with 2.6 mm sample in reference beam.

From the data of the transmission measurements we have derived the attenuation length of the material 31 ± 5 cm at the wavelength of CdWO_4 emission maximum 480 nm [21]. At 400 nm the attenuation lengths of the samples are 5.8 cm (No. 1), 5.2 cm (No. 2) and 4.1 cm (No. 3). One

can explain the decrease of transmittance for the samples distant from the beginning of the crystal growth by the well known effect of defects increase during CdWO_4 crystal growth.

After the low background measurements (see below subsection 4.2) the crystals No. 1 and 2 were annealed at the temperature $\approx 870^\circ\text{C}$ over 55 hours. The annealing improved transmittance of the samples in the region of wavelengths 350 – 420 nm on 10 – 40 % (see Fig. 2).

3.3 Energy resolution

To measure the scintillation properties, the samples No. 1 and 2 were optically coupled with the help of Dow Corning Q2-3067 optical couplant to 3" photomultiplier (PMT) Philips XP2412. To improve scintillation light collection, the crystals were wrapped by a few layers of polytetrafluoroethylene (PTFE) tape. The measurements were carried out with 10 μs shaping time of ORTEC 575 spectroscopy amplifier to collect most of the charge from the anode of the PMT. The detectors were irradiated by γ quanta of ^{137}Cs , ^{207}Bi and ^{232}Th sources. Fig. 3 shows the pulse amplitude spectra measured with the $^{116}\text{CdWO}_4$ crystal scintillator No. 2. The energy resolution 11.1% and 10.1% (FWHM) were obtained for the 662 keV γ line of ^{137}Cs with the detectors No. 1 and 2, respectively. The energy resolution for 2615 keV γ line of ^{232}Th source is 7.1% and 6.7% for the scintillators No. 1 and 2, respectively.

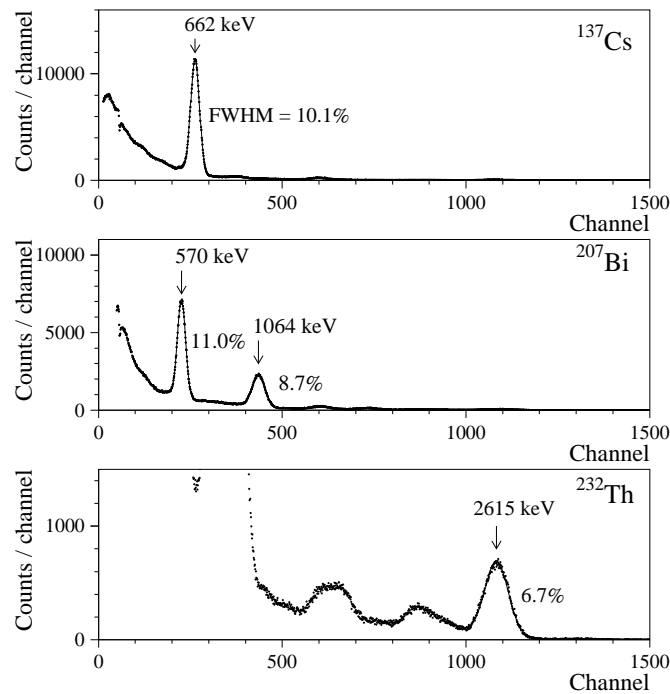


Figure 3. The energy spectra of ^{137}Cs , ^{207}Bi and ^{232}Th γ quanta measured by the $^{116}\text{CdWO}_4$ scintillation crystal No. 2.

After the annealing at high temperature the energy resolution of the crystals was improved (see subsection 4.2).

4. Low background measurements, results and discussion

4.1 Measurements with ultra-low background HPGe γ ray spectrometry

The $^{116}\text{CdWO}_4$ crystal No. 3 was measured for 788 h with the ultra-low background HPGe γ ray spectrometer GeCris (volume 468 cm^3 , 120% relative efficiency). The background data were accumulated over 1046 h (see Fig. 4). In order to determine the radioactive contamination of the sample, the detection efficiencies were calculated using Monte Carlo simulation based on the GEANT4 software package [22]. Peaks in the spectra are due to the naturally occurring radionuclides of the uranium and thorium chains and ^{40}K . Only upper limits could be obtained for corresponding activities. We have detected low contamination by ^{137}Cs and ^{207}Bi in the crystal on the level of 2.1(5) mBq/kg and 0.6(2) mBq/kg, respectively. In addition, we have observed peaks of ^{44}Ti (67.9 keV and 78.4 keV, the half-life of ^{44}Ti is 60 yr) and its daughter ^{44}Sc (1157.0 keV) in the data accumulated with the $^{116}\text{CdWO}_4$ crystal. However, the peaks are due to contamination of the HPGe detector (not the crystal scintillator sample) by ^{44}Ti . Indeed the detector, before the run with the $^{116}\text{CdWO}_4$ sample, has been used to measure a sample of titanium with rather high activity of ^{44}Ti . Limits on mBq/kg level were obtained for other potential contaminations. The results of the measurements are presented in Table 3.

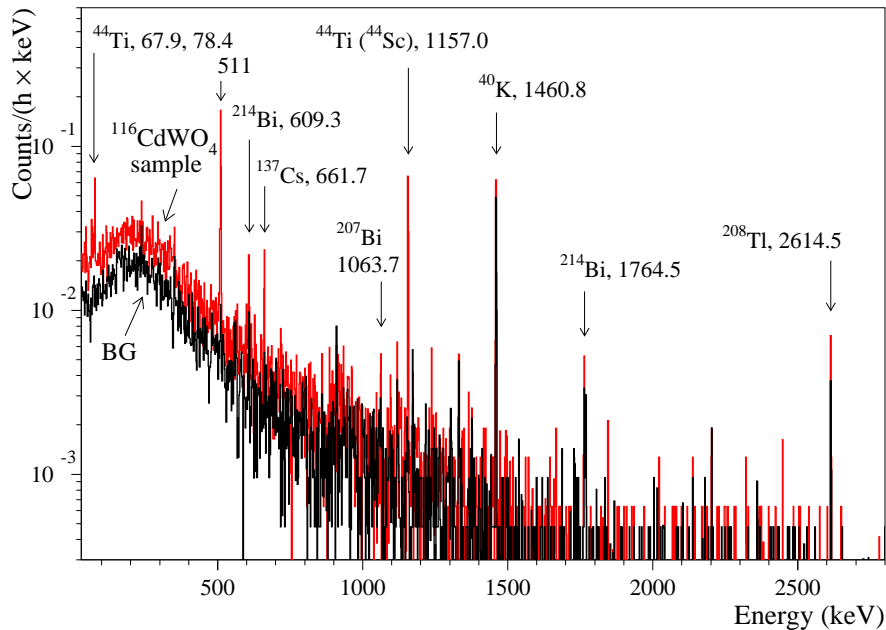


Figure 4. (Color online) Energy spectra measured with the 325.6 g $^{116}\text{CdWO}_4$ sample over 788 h and without sample over 1046 h (BG) by ultra-low background HPGe γ spectrometer. Some excess of the spectrum accumulated with the $^{116}\text{CdWO}_4$ sample is due to an accidental contamination of the HPGe detector by radioactive ^{44}Ti . The energy of the γ lines are in keV.

4.2 Low background detector system with $^{116}\text{CdWO}_4$ crystal scintillators

The $^{116}\text{CdWO}_4$ crystal scintillators No. 1 and 2 were fixed inside the cavities $\varnothing 47 \times 61$ mm in

the central part of the polystyrene based plastic scintillator light-guides (UPS923A, Amcrys-H, Ukraine), 70 mm in diameter and 194 mm in length (a schematic view of the set-up is presented in Fig. 5). The cavities were filled with liquid scintillator (LS-221, Institute for Scintillation Materials, Kharkiv, Ukraine) which does not affect the polystyrene scintillator. The scintillating light-guides act as active veto. A significant difference of CdWO_4 pulse-shape (effective average decay time is $13 \mu\text{s}$ [21]) in comparison to much faster plastic and liquid scintillators signals (few nanoseconds) offers the possibility to exploit the discrimination of the light-guide signals. Each plastic light-guide was optically connected on opposite sides to two high purity quartz light-guides $\varnothing 70 \times 200$ mm each. Two low radioactive 3" diameter PMTs Hamamatsu R6233MOD viewed each detector from opposite sides. The light-guides are wrapped by a few layers of PTFE reflection tape. All the optical contacts between the light-guides and PMTs were provided by Dow Corning Q2-3067 optical couplant. The detectors with the $^{116}\text{CdWO}_4$ crystals were placed between two polystyrene based plastic scintillators (UPS89, Amcrys-H, Ukraine) $500 \times 300 \times 120$ mm. A channel $\varnothing 14 \times 200$ mm was made (in the middle of the upper plastic scintillator of its width, 51 mm from the above edge of the plastic) to insert radioactive sources. Two low background 3" diameter PMTs ETL 9302FLA were optically connected to the plastic scintillators.

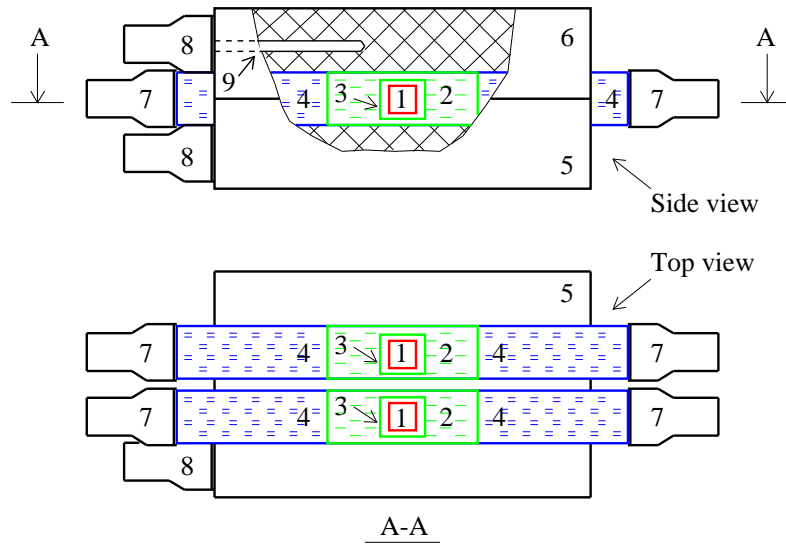


Figure 5. (Color online) Low background scintillation detector. (1) $^{116}\text{CdWO}_4$ crystals scintillators, (2) plastic scintillator light-guides, (3) cavities in the light-guides filled by liquid scintillator, (4) quartz light-guides, (5, 6) plastic scintillators, (7) four PMTs Hamamatsu R6233MOD, (8) two PMTs ETL 9302FLA, (9) channel $\varnothing 14 \times 200$ mm in the plastic scintillator 6 to insert radioactive sources.

The detector system was installed deep underground in the low background DAMA/R&D set-up at the Gran Sasso National Laboratories of the INFN (Italy). The detector system was surrounded by Cu bricks and sealed in a low radioactive air-tight Cu box continuously flushed by high purity nitrogen gas (stored deeply underground for a long time) to avoid the presence of residual environmental radon. The Cu box was surrounded by a passive shield made of high purity Cu, 10 cm of thickness, 15 cm of low radioactive lead, 1.5 mm of cadmium and 4 to 10

cm of polyethylene/paraffin to reduce the external background. The shield was contained inside a Plexiglas box, also continuously flushed by high purity nitrogen gas.

An event-by-event data acquisition system based on a 1 GS/s 8 bit transient digitizer (Acqiris DC270) records the time of each event and the pulse shape over a time window of 100 μ s from the $^{116}\text{CdWO}_4$ detectors (the sum of the signals from two PMTs), the plastic scintillator, and the sum of signals from the $^{116}\text{CdWO}_4$ scintillators attenuated to provide an energy scale up to ≈ 10 MeV (the electronic chain of the detector system is briefly summarized in Fig. 6). Taking into account the slow kinetics of the CdWO_4 scintillation decay, the sampling frequency of the transient digitizer was set to 20 MS/s. An especially developed electronic unit (SST-09) provides triggers for cadmium tungstate scintillation signals. The unit rejects PMT noise, plastic scintillator light-guide signals and CdWO_4 events with large admixture of the plastic. Further rejection of the plastic overlaps can be realized off line by the pulse-shape analysis described below.

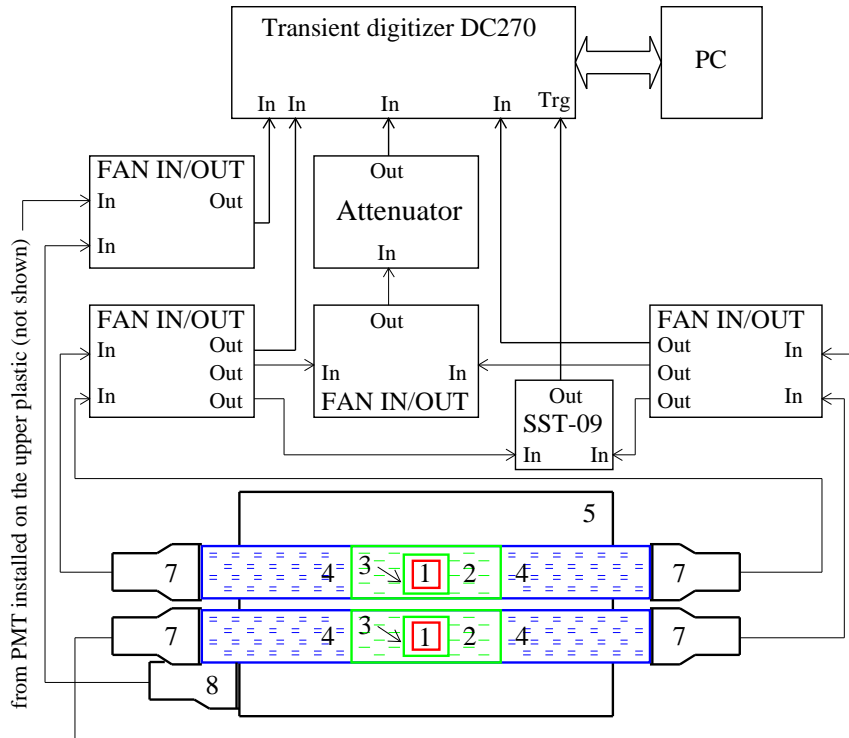


Figure 6. (Color online) Schema of the electronic chain (details of the low background detector are denoted in Fig. 5). (FAN IN/OUT) Linear FAN-IN/FAN-OUT, LeCroy Model 428F; (SST-09) home made electronic unit to provide triggers for cadmium tungstate scintillation signals; (Attenuator) Dual attenuator, CAEN model No 110; (PC) personal computer. Inputs and outputs of the electronic units are denoted as "In" and "Out", respectively; "Trg" denotes a trigger input of the transient digitizer.

The energy scale and resolution of the detector system was tested with ^{22}Na , ^{60}Co , ^{137}Cs and ^{228}Th γ sources. The energy resolution of the $^{116}\text{CdWO}_4$ detectors before the annealing can be described by functions: $\text{FWHM}_{\gamma 1} = \sqrt{10.5 \times E_{\gamma}}$, and $\text{FWHM}_{\gamma 2} = \sqrt{540 + 8.5 \times E_{\gamma}}$ for the detectors No. 1 and 2, respectively (here E_{γ} and FWHM_{γ} are in keV). The energy scale and resolution of

the detectors were tested once during the measurements and at the end of the experiment with the help of ^{22}Na γ source inserted into the set-up through the special channel without switching off the high voltage of the PMTs. We have observed neither shift of the energy scale nor degradation of the energy resolution of the detectors during almost 2.5 months of low background measurements.

As a result of the annealing of the $^{116}\text{CdWO}_4$ crystal scintillators performed after the low background measurements, the energy resolution of the detectors for the 2615 keV γ line of ^{228}Th was improved from 6.9% to 5.3% for the detector with the crystal No. 1, and from 6.2% to 5.0% for the detector No. 2. Energy spectra accumulated with the $^{116}\text{CdWO}_4$ detector No. 2 after the annealing are presented in Fig. 7.

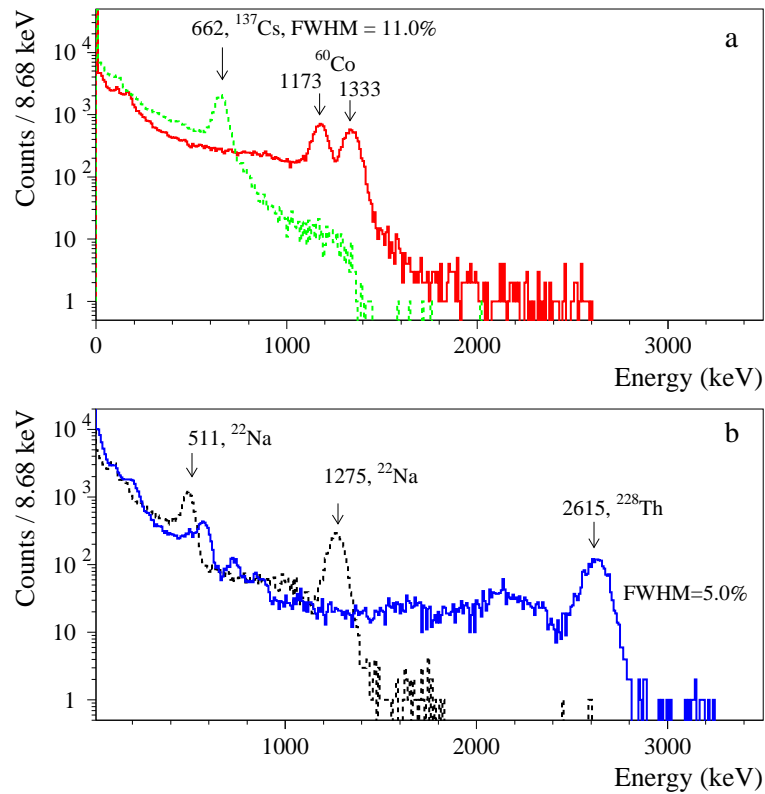


Figure 7. (Color online) Energy spectra accumulated by the $^{116}\text{CdWO}_4$ detector No. 2 with ^{137}Cs , ^{60}Co (a), ^{22}Na and ^{228}Th γ sources (b) in the low background set-up after annealing of the crystals. Energies of γ lines are in keV.

4.3 Data analysis

The energy spectra accumulated with the $^{116}\text{CdWO}_4$ detectors over 1727 h of low background measurements are presented in Fig. 8. The spectra are rather similar with a small difference in the region 0.6 – 1.2 MeV where α particles from U/Th are observed (see Subsection 4.3.1 describing a pulse-shape discrimination to select α particles). The counting rate of 0.26 count/s in the energy interval 0.08 – 0.6 MeV is mainly due to the decay of ^{113}Cd ($Q_\beta = 320$ keV, $T_{1/2} = 8.04 \times 10^{15}$ yr)

with the activity (0.10 ± 0.01) Bq/kg¹ and $^{113\text{m}}\text{Cd}$ ($Q_\beta = 583$ keV, $T_{1/2} = 14.1$ yr) with the activity (0.46 ± 0.02) Bq/kg.

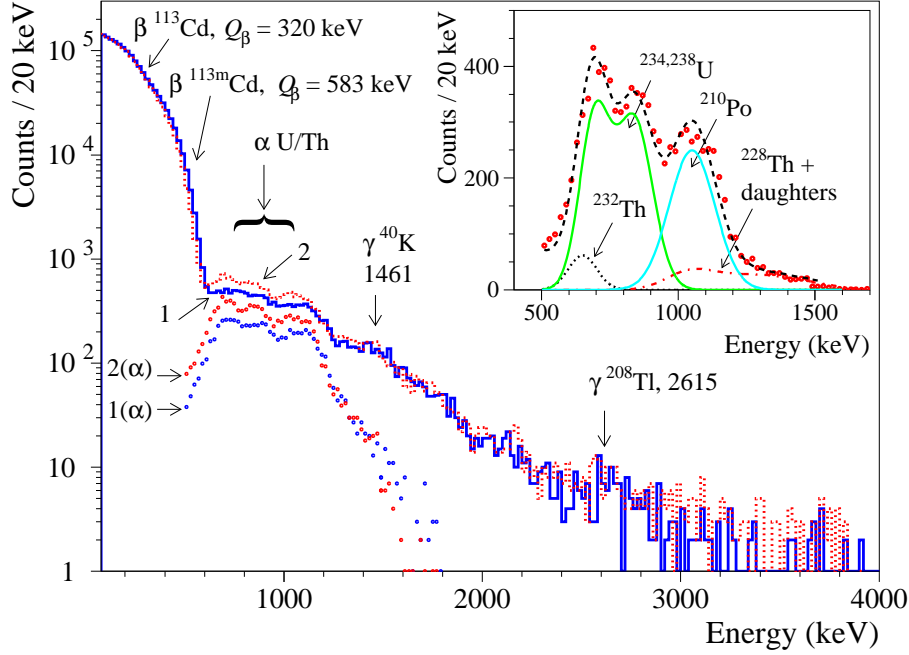


Figure 8. (Color online) The energy spectra accumulated with the $^{116}\text{CdWO}_4$ crystal scintillators No. 1 and 2 in the low background DAMA/R&D set-up over 1727 h. The energy spectra of α events selected by the pulse-shape discrimination (see text) are also shown. Some difference in the data in the energy region 0.6 – 1.2 MeV visible both in the raw data and in the spectra of α events is due to higher α activity of U/Th daughters’ traces in the crystal No. 2. In the inset, the α spectrum of the detector No. 2 is depicted together with the model, which includes α decays from ^{238}U and ^{232}Th families.

Contributions to the background above the energy 0.6 MeV were analyzed by the pulse-shape discrimination and the time-amplitude techniques.

4.3.1 Pulse-shape discrimination

To select γ quanta (β particles) and α particles, the data of the low background measurements were analyzed by using the optimal filter method proposed by E. Gatti and F. De Martini [23] (see also [24] where the analysis was developed for CdWO_4 crystal scintillators). For each experimental signal, the numerical characteristic of its shape (shape indicator, SI) was defined as $SI = \sum f(t_k) \times P(t_k) / \sum f(t_k)$, where the sum is over time channels k , starting from the origin of the signal and up to 30 μs , $f(t_k)$ is the digitized amplitude (at the time t_k) of a given signal. The weight function $P(t)$ is defined as: $P(t) = \{\bar{f}_\alpha(t) - \bar{f}_\gamma(t)\} / \{\bar{f}_\alpha(t) + \bar{f}_\gamma(t)\}$, where the reference pulse shapes $\bar{f}_\alpha(t)$ and $\bar{f}_\gamma(t)$ are taken from [21]. The pulse-shape discrimination of the events accumulated in the low background measurements with the $^{116}\text{CdWO}_4$ detector No. 1 is demonstrated in Fig. 9. Alpha events were selected from the accumulated data (see the energy spectra of α particles in Inset of

¹The activity is calculated on the basis of the isotopic abundance and the half-life of ^{113}Cd .

Fig. 8), which allow to estimate the total internal α activity of U/Th as 1.9(2) mBq/kg and 2.7(3) mBq/kg in the $^{116}\text{CdWO}_4$ crystal scintillators No. 1 and 2, respectively. Slightly higher α activity in the sample No. 2 can be explained by accumulation of U/Th daughters' traces in the melt during the crystal growth.

To estimate the activity of the α active nuclides from the U/Th families in the crystals, the energy spectra of the α events were fitted in the energy interval 0.5 – 1.5 MeV by using a simple model: ten Gaussian functions to describe α peaks of ^{232}Th (and its daughters: ^{228}Th , ^{224}Ra , ^{220}Rn , ^{216}Po , ^{212}Bi), ^{238}U (and its daughters: ^{234}U , ^{230}Th , ^{210}Po) plus exponential function (to describe background). Fit of the α spectrum accumulated with the detector No. 2 is shown in Inset of Fig. 8. Because of the worse energy resolution for α particles in comparison to γ quanta in CdWO_4 scintillation detectors [14], we conservatively give limits on activities of ^{232}Th and ^{238}U , ^{230}Th , ^{210}Po (expected to be not in equilibrium with ^{238}U) in the $^{116}\text{CdWO}_4$ scintillators. The data obtained from the fits are presented in Table 3.

In addition, the optimal filter method allows to distinguish and reject from the data also overlapping of plastic scintillator's pulses with $^{116}\text{CdWO}_4$ signals, random coincidence of events, some events from the fast chain of decays $^{212}\text{Bi} \rightarrow ^{212}\text{Po} \rightarrow ^{208}\text{Pb}$ (^{232}Th family).

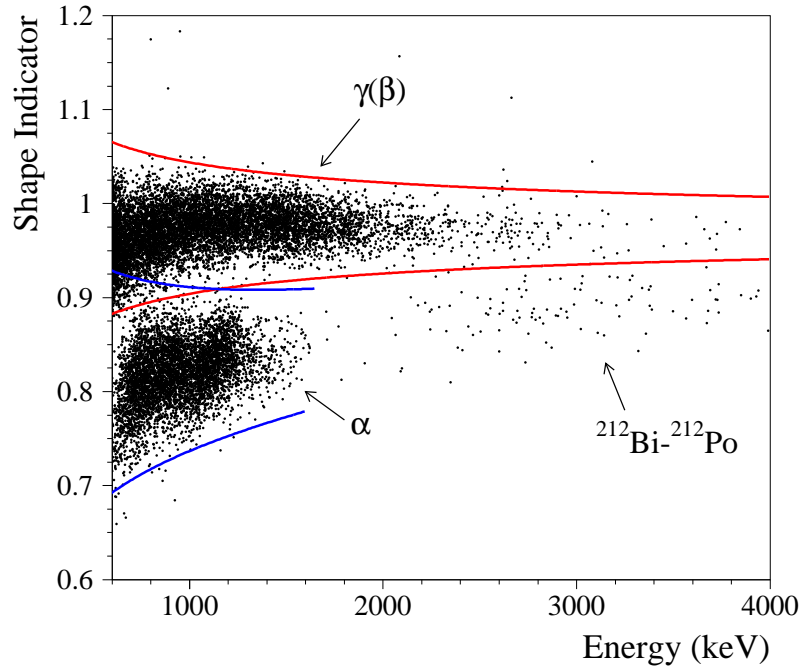


Figure 9. (Color online) Shape indicators (see text) versus energy for background exposition over 1727 h with $^{116}\text{CdWO}_4$ crystal scintillator No. 1 in the low background set-up. Three sigma intervals for shape indicator values corresponding to γ quanta (β particles) and α particles are drawn.

4.3.2 Time-amplitude analysis of ^{228}Th and ^{227}Ac contaminations

Activities of ^{228}Th (^{232}Th family) and ^{227}Ac (^{235}U) in the $^{116}\text{CdWO}_4$ crystal scintillators were estimated by the time-amplitude analysis of the events accumulated in the low background mea-

surements. The technique of the time-amplitude analysis is described in detail in [7, 25, 26].

To determine the activity of ^{228}Th , the following sequence of α decays was selected: ^{224}Ra ($Q_\alpha = 5.789$ MeV, $T_{1/2} = 3.66$ d) \rightarrow ^{220}Rn ($Q_\alpha = 6.405$ MeV, $T_{1/2} = 55.6$ s) \rightarrow ^{216}Po ($Q_\alpha = 6.907$ MeV, $T_{1/2} = 0.145$ s) \rightarrow ^{212}Pb . The obtained α peaks and the distributions of the time intervals between events (see Fig. 10) are in agreement with those expected for α particles of the chain. Taking into account the efficiencies in the time windows to select $^{220}\text{Rn} \rightarrow ^{216}\text{Po} \rightarrow ^{212}\text{Pb}$ events (94.5%), the activities of ^{228}Th in the crystals No. 1 and 2 were calculated as 0.057(7) mBq/kg and 0.062(6) mBq/kg, respectively.

By using positions of the three α peaks in the γ scale of the detector we have obtained the following dependence of α/β ratio on energy of α particles E_α : $\alpha/\beta = 0.113(6) + 0.132(10) \times 10^{-4} E_\alpha$ in the energy interval 5.8 – 6.9 MeV (E_α is in keV).

The same approach was used to search for the chain ^{223}Ra ($Q_\alpha = 5.979$ MeV, $T_{1/2} = 11.44$ d) \rightarrow ^{219}Rn ($Q_\alpha = 6.946$ MeV, $T_{1/2} = 3.96$ s) \rightarrow ^{215}Po ($Q_\alpha = 7.526$ MeV, $T_{1/2} = 1.78$ ms) \rightarrow ^{211}Pb from the ^{235}U family. Limit on activities of ^{227}Ac in the crystals No. 1 and 2 was obtained on the level of ≤ 0.002 mBq/kg.

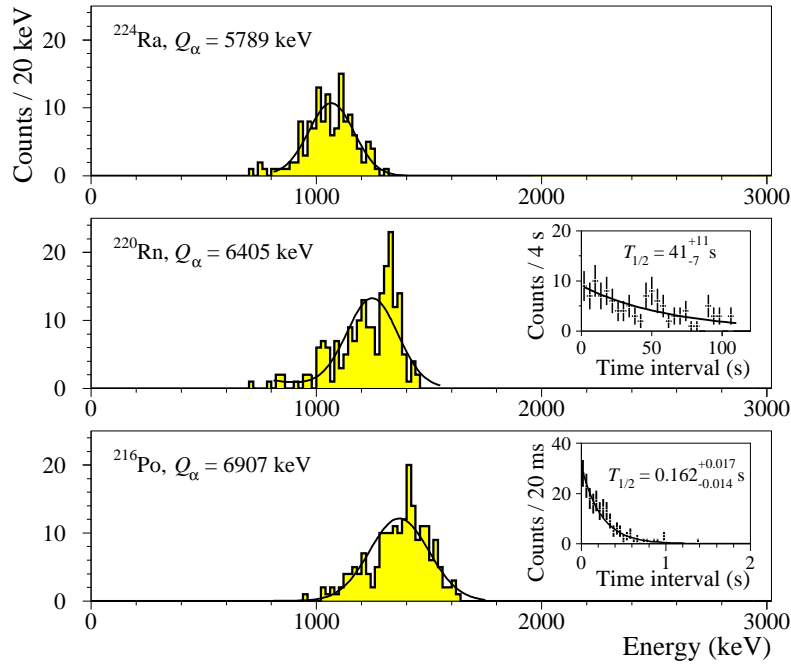


Figure 10. (Color online) Alpha peaks of ^{224}Ra , ^{220}Rn and ^{216}Po selected by the time-amplitude analysis from the data accumulated during 1727 h with the $^{116}\text{CdWO}_4$ detector No. 1. The obtained half-lives of ^{220}Rn (41_{-7}^{+11} s) and ^{216}Po ($0.162_{-0.014}^{+0.017}$ s) are in agreement with the table values (55.6 s and 0.145 s, respectively [27]).

4.3.3 Selection of Bi–Po events

Double pulses from the decays of ^{214}Bi ($Q_\beta = 3.272$ MeV) \rightarrow ^{214}Po ($Q_\alpha = 7.833$ MeV, $T_{1/2} = 164$ μs) \rightarrow ^{210}Pb (daughters of ^{226}Ra from the ^{238}U family) were searched for. One event in the data

accumulated with both detectors was found. Therefore, taking into account the efficiency of the Bi-Po events selection in the time interval of the analysis $1 - 75 \mu\text{s}$ (26.7%), we set limit on ^{226}Ra activity in the crystals No. 1 and 2 as $\leq 0.005 \text{ mBq/kg}$.

A summary of the radioactive contamination of the $^{116}\text{CdWO}_4$ crystal scintillators is presented in Table 3.

Table 3. Radioactive contamination of $^{116}\text{CdWO}_4$ crystal scintillators. Data for CdWO_4 [13], $^{116}\text{CdWO}_4$ [14, 7], and $^{106}\text{CdWO}_4$ [11] are given for comparison.

Chain	Nuclide (Sub-chain)	Activity (mBq/kg)					
		$^{116}\text{CdWO}_4$		CdWO_4	$^{116}\text{CdWO}_4$	$^{106}\text{CdWO}_4$	
		No. 1	No. 2	No. 3	[13]	[14, 7]	[11]
	^{40}K			≤ 26	≤ 5	0.3(1)	≤ 11
	^{60}Co			≤ 0.47	≤ 0.4		
	$^{110\text{m}}\text{Ag}$	0.06(4)	0.06(4)				
	^{113}Cd	100(10)	100(10)		558(4)	91(5)	174
	$^{113\text{m}}\text{Cd}$	460(20)	460(20)		≤ 3.4	1.1(1)	112000(5000)
	^{137}Cs			2.1(5)	≤ 0.3	0.43(6)	
	^{207}Bi			0.6(2)			1.3(3)
^{232}Th	^{232}Th	≤ 0.08	≤ 0.08		≤ 0.026	0.053(9)	≤ 0.1
	^{228}Th	0.057(7)	0.062(6)	≤ 2.0	0.008(4)	0.039(2)	0.053(5)
^{235}U	^{235}U			≤ 4.0			
	^{227}Ac	≤ 0.002	≤ 0.002		0.014(9)	0.0014(9)	
^{238}U	^{238}U	≤ 0.4	≤ 0.6		≤ 0.045	≤ 0.6	≤ 0.3
	$^{234\text{m}}\text{Pa}$			≤ 58		≤ 0.2	
	^{230}Th	≤ 0.06	≤ 0.05			≤ 0.5	≤ 0.8
	^{226}Ra	≤ 0.005	≤ 0.005	≤ 2.6	≤ 0.018	≤ 0.004	≤ 0.3
	^{210}Pb			≤ 15000		≤ 0.4	
	^{210}Po	≤ 0.4	≤ 0.6		≤ 0.063		≤ 0.3
	Total α activity	1.9(2)	2.7(3)		0.26(4)	1.40(10)	2.1(1)

Selection of double pulses produced by the fast chain of the decays ^{212}Bi ($Q_\beta = 2.254 \text{ MeV}$) \rightarrow ^{212}Po ($Q_\alpha = 8.954 \text{ MeV}$, $T_{1/2} = 0.299 \mu\text{s}$) \rightarrow ^{208}Pb (^{232}Th family) was developed. An example of such an event pulse-shape and the result of the selection for the $^{116}\text{CdWO}_4$ crystal scintillator No. 1 are presented in Fig. 11. The analysis gives the activity of ^{212}Bi (which is in equilibrium with ^{228}Th) 0.054(5) mBq/kg (crystal No. 1) and 0.095(6) mBq/kg (crystal No. 2) in a reasonable agreement with the results of the time-amplitude analysis.

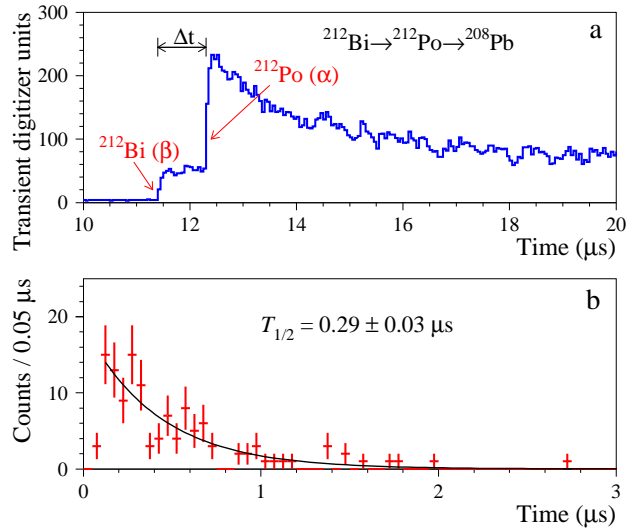


Figure 11. (Color online) (a) Example of $^{212}\text{Bi} \rightarrow ^{212}\text{Po} \rightarrow ^{208}\text{Pb}$ event in the $^{116}\text{CdWO}_4$ scintillator. (b) The time distribution for the fast sequence of β (^{212}Bi) and α (^{212}Po) decays selected by the pulse-shape and the front edge analyses from the background data accumulated with the $^{116}\text{CdWO}_4$ detector No. 1 over 1727 h. The fit of the time distribution gives a half-life $T_{1/2} = (0.29 \pm 0.03) \mu\text{s}$ which is in good agreement with the table value for ^{212}Po ($0.299 \mu\text{s}$ [27]).

4.4 Background in the region of $Q_{\beta\beta}$ of ^{116}Cd

By using the pulse-shape and the front edge analyses we can substantially reduce the background of the detector in the energy region of interest near 2.8 MeV where a peak of neutrinoless double β decay of ^{116}Cd is expected (see Fig. 12). The counting rate of the detector after removing the part of data accumulated during first 17 days of measurements (to avoid effects of radon and cosmogenic activation) in the energy interval of interest 2700 – 2900 keV is 0.28 counts/(yr \times keV \times kg).

A certain contribution to the background ≈ 0.1 counts/(yr \times keV \times kg) in the energy interval 2.7 – 2.9 MeV comes from the 2615 keV peak caused by external γ quanta from the decays of ^{208}Tl (daughter of ^{232}Th). Contamination of the set-up (first of all of PMTs, cables, quartz light-guides, copper shield) by thorium can be a source of the background. We are going to simulate ^{208}Tl decays to estimate the contribution from different parts of the set-up. Our preliminary calculations show that the PMTs and quartz light-guides can be the main sources of the 2615 keV peak. We are going to apply ultra-low background HPGe γ ray spectrometry to measure radioactive contamination of the PMTs and sample of the quartz.

The two neutrino mode of 2β decay of ^{116}Cd (assuming a half-life $T_{1/2}^{2\nu} = 2.8 \times 10^{19}$ yr [28]) contributes 0.00045 counts/(yr \times keV \times kg) in the energy interval 2.7 – 2.9 MeV.

One of the major sources of the detector background in the energy region of the expected $0\nu 2\beta$ peak of ^{116}Cd is contamination of the $^{116}\text{CdWO}_4$ crystals by ^{208}Tl . The Monte Carlo simulation of internal ^{208}Tl (see Fig. 12, c) gives about ≈ 0.09 counts/(yr \times keV \times kg) in the region of interest. We consider as a possibility the crystals recrystallization to reduce the thorium contamination. To our knowledge there is no data in literature about segregation of thorium to CdWO_4 crystals.

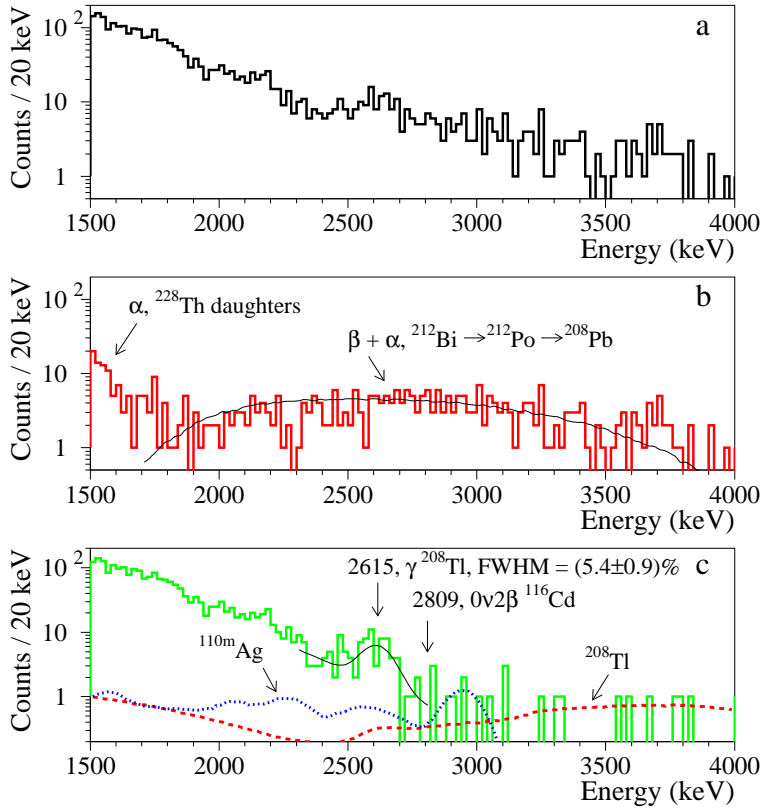


Figure 12. (Color online) (a) Initial sum spectrum of the two $^{116}\text{CdWO}_4$ detectors measured over 1322 h (total exposure 1554 kg \times h) in anti-coincidence with the plastic scintillation counter and the active light-guides; (b) the spectra of α and $\beta + \alpha$ events selected by using the pulse-shape and the front edge analyses (see text) together with the simulated response function for the $^{212}\text{Bi} \rightarrow ^{212}\text{Po} \rightarrow ^{208}\text{Pb}$ decay chain; (c) β and γ events selected with the help of the pulse-shape and the front edge analyses (the efficiency of the selection procedure for γ quanta / β particles is 95%). The fit of the ^{208}Tl γ peak with the energy 2615 keV is shown by solid line. The Monte Carlo simulated energy spectra of internal ^{110m}Ag and ^{208}Tl in the $^{116}\text{CdWO}_4$ crystals are presented.

A positive result of recrystallization procedure can be reached if the segregation coefficient for thorium is much less than 1. To determine the segregation of thorium in CdWO_4 , we are going to measure the activity of ^{228}Th in the $^{116}\text{CdWO}_4$ crystal No. 3 by the scintillation method. Besides we are going to measure the activity of ^{228}Th in the rest of the melt after the crystal growth by ultra-low background HPGe γ ray spectrometry, and concentration of ^{232}Th by the High Resolution Inductively Coupled Plasma Mass Spectrometry. Higher concentration of thorium in the rest will be an indication of low segregation of thorium in CdWO_4 crystal. Then the crystal No. 3 can be recrystallized and measured by the low counting scintillation method to estimate activity of ^{228}Th .

In case of positive result all the crystals can be recrystallized. In case of not enough high efficiency of the recrystallization to reduce thorium, one could recover the enriched cadmium from

the crystals and scraps, purify by physical (vacuum distillation and filtering)² and chemical (by coprecipitation on a collector) methods, and grow crystal again. Output of purified materials can be decreased to reach deeper purification of enriched cadmium. It should be stressed that a satisfactory radiopurity level (activity of ^{228}Th less than 0.01 mBq/kg) was reached in some samples of CdWO_4 crystals [8, 13]. Besides, very high level of radiopurity (~ 0.002 mBq/kg of ^{228}Th) was detected in zinc tungstate (ZnWO_4) crystal scintillators [29], which have chemical and physical properties rather similar to CdWO_4 . An encouraging result of recrystallization was reported recently for calcium tungstate (CaWO_4) crystal scintillators [30]. One could also expect improvement of the crystal scintillators quality thanks to deep purification of initial materials and recrystallization. Therefore contribution from the 2615 keV peak could be suppressed further.

It should be also mentioned a “natural” way of the background decrease during next few years due to the decay of the trace ^{228}Th in the $^{116}\text{CdWO}_4$ crystals (assuming broken equilibrium of ^{232}Th chain and lower activity of ^{228}Ra in comparison to ^{228}Th and ^{232}Th). Such an effect (decrease of the ^{228}Th activity in the $^{116}\text{CdWO}_4$ crystals) was observed in the Soltovina experiment [7].

Finally, we assume that the essential part of the background beyond the 2615 keV peak is due to cosmogenic activation of the $^{116}\text{CdWO}_4$ crystals by ^{110m}Ag ($Q_\beta = 3.0$ MeV; $T_{1/2} = 250$ d) [31], which can provide background up to 3 MeV. Moreover, radioactive isotope ^{110m}Ag with activity 0.4 mBq/kg was observed in [15] in the enriched cadmium 116 used to produce the scintillators. Our assumption was justified by the Monte Carlo simulation of the $^{116}\text{CdWO}_4$ detector response to internal ^{110m}Ag . A simulated model of ^{110m}Ag corresponding to activity 0.06 mBq/kg is shown in Fig. 12, c. Another possible cosmogenic radionuclide in the $^{116}\text{CdWO}_4$ crystals can be ^{106}Ru ($Q_\beta = 40$ keV; $T_{1/2} = 374$ d) \rightarrow ^{106}Rh ($Q_\beta = 3.5$ MeV; $T_{1/2} = 30$ s) [31]. However, cosmogenic background is expected to be reduced substantially due to decay of cosmogenic radionuclides, in particular of ^{110m}Ag .

Now the experiment is in progress with an improved energy resolution after the annealing of the crystals. We expect to improve the background reduction at this stage of experiment thanks to more careful pulse-shape analysis to reject events caused by ^{228}Th daughters. In particular, we use now a higher resolution of the transient digitizer (50 Ms/s instead of 20 Ms/s) to suppress further the background caused by the fast sequence $^{212}\text{Bi} \rightarrow ^{212}\text{Po} \rightarrow ^{208}\text{Pb}$. In addition, we are developing the analysis of the sequence of the decays ^{212}Bi ($Q_\alpha = 6.207$ MeV, $T_{1/2} = 60.55$ m) \rightarrow ^{208}Tl ($Q_\beta = 5.001$ MeV, $T_{1/2} = 3.053$ m) \rightarrow ^{208}Pb to reject events of ^{208}Tl decay. Contribution from the 2615 keV γ line is expected to be reduced to ≈ 0.06 counts/(yr \times keV \times kg) thanks to the improvement of the energy resolution.

5. Monte Carlo simulation of double β decay of ^{116}Cd , estimations of experimental sensitivity

The computer simulation of the different radioactive processes in the scintillation low background detector with $^{116}\text{CdWO}_4$ scintillators in the 4π active shielding has been performed with EGS4 package [32]. The initial kinematics of the particles emitted in the decay of the nuclei was given by

²Unfortunately, only part of the enriched cadmium 116 was purified by the vacuum distillation and filtering (see subsection 2.3).

an event generator DECAY0 [33]. The following double β processes in ^{116}Cd have been simulated: $0\nu 2\beta$ and $2\nu 2\beta$ decay to the ground state and to the five lowest excited levels of ^{116}Sn ; neutrinoless double β decay with emission of one, two and bulk [34] majoron(s). Approximately 3 – 9 millions of decays were simulated for the different channels of ^{116}Cd 2β decay. The calculated distributions are shown in Fig. 13. In particular, the calculations give the detection efficiency in a peak of the neutrinoless double β decay of ^{116}Cd as 89% (one can compare with the value of 83% in the Solotvina experiment [7] where the crystals of the smaller volume were used).

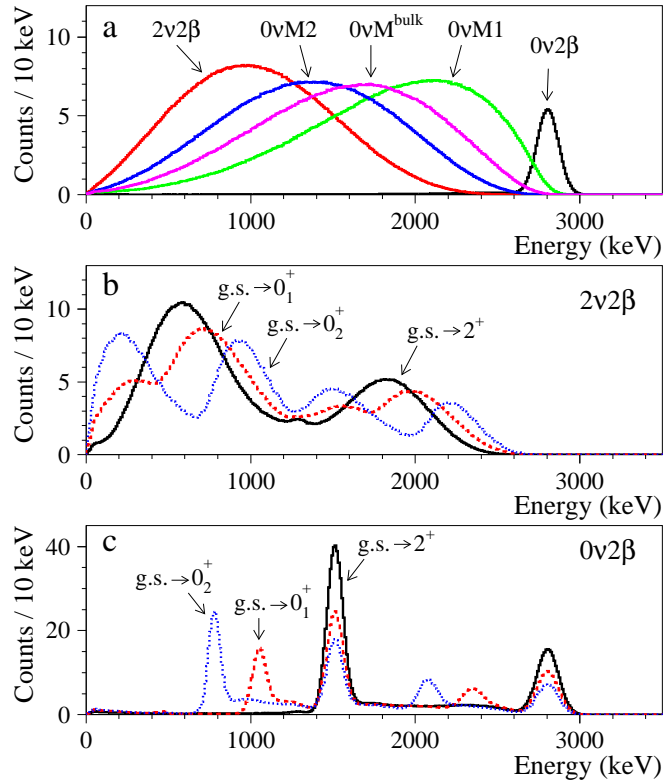


Figure 13. (Color online) Simulated response functions of the $^{116}\text{CdWO}_4$ detector for the different modes of double β decay of ^{116}Cd to the ground state of ^{116}Sn (a); Simulated distributions of the detector for two neutrino (b) and neutrinoless (c) decay of ^{116}Cd to the excited levels of ^{116}Sn . Approximately 3 – 9 millions of decays were simulated for the different decay channels. The distributions are normalized to 1000 decays, except the $0\nu 2\beta$ mode, which is normalized to 100 decays.

On the basis of the detection efficiency and of the number of ^{116}Cd nuclei in the two $^{116}\text{CdWO}_4$ crystal scintillators No. 1 and 2 (1.6×10^{24}), assuming decrease of the detector background to the level of 0.01 – 0.1 counts/(yr \times keV \times kg) (expected due to the decay of cosmogenic radionuclides, improvement of the energy resolution and the pulse-shape analysis, possible change of the most contaminated parts of the set-up and reduction of ^{228}Th activity after recrystallization of the $^{116}\text{CdWO}_4$ crystals), one can estimate the sensitivity of a 5 years experiment to the $0\nu 2\beta$ decay of ^{116}Cd as $T_{1/2} \sim (0.5 - 1.5) \times 10^{24}$ yr. According to the recent calculations of matrix elements [4, 5, 6], these half-lives correspond to the effective neutrino mass $\langle m_\nu \rangle \approx 0.4 - 1.4$ eV, which is

on the level of the most sensitive 2β experiments.

6. Conclusions

Cadmium tungstate crystal scintillators were developed from cadmium enriched in ^{116}Cd for a high sensitivity experiment to search for double beta decay of ^{116}Cd . Samples of enriched cadmium were purified by chemical methods, the most polluted part was additionally purified by vacuum distillation. Some part of the enriched material was recovered from scraps after enriched $^{116}\text{CdWO}_4$ crystal growth in 1988. Cadmium tungstate compounds were synthesized from solutions. A $^{116}\text{CdWO}_4$ crystal boule with mass of 1868 g (which is 87% of the initial charge) was grown by the low-thermal-gradient Czochralski technique. Two $^{116}\text{CdWO}_4$ crystal scintillators (586 g and 589 g) produced from the boule show an energy resolution FWHM $\approx 7\%$ (for 2615 keV γ line of ^{208}Tl) in measurements with the crystals directly viewed by photomultiplier.

The absolute isotopic composition of ^{116}Cd in the crystal was determined as 82% by mass-spectrometry. Thanks to the careful purification of the initial materials and using the low-thermal-gradient Czochralski technique, the crystal has rather high transmittance: the attenuation length is 31 ± 5 cm at the wavelength of CdWO_4 emission maximum 480 nm. After the low background measurements the crystals No. 1 and 2 were annealed at the temperature ≈ 870 °C over 55 hours. The annealing improved transmittance of the samples in the region of wavelengths 350 – 420 nm on 10 – 40 %.

The low background detector system with two enriched $^{116}\text{CdWO}_4$ crystal scintillators (586 g and 589 g) was installed in the underground Gran Sasso National Laboratories of the INFN (Italy). The energy resolution of the detector with $^{116}\text{CdWO}_4$ crystal scintillators inside the plastic scintillator light-guides with length of 28 cm was even slightly better than that in the case when the scintillators were directly viewed by a photomultiplier. Furthermore the energy resolution was improved to $\approx 5\%$ (for 2615 keV γ line of ^{208}Tl) after the annealing of the $^{116}\text{CdWO}_4$ crystals.

The low background measurements over 1727 h allowed to estimate radioactive contamination of the $^{116}\text{CdWO}_4$ scintillators. In addition the radioactive contamination of another $^{116}\text{CdWO}_4$ sample (326 g) was tested with the help of ultra-low background HPGe γ ray spectrometry. The activities of ^{226}Ra and ^{228}Th , which are the most dangerous isotopes for double β decay experiments, are on the level < 0.005 mBq/kg and ≈ 0.06 mBq/kg, respectively.

By using the pulse-shape discrimination of the ^{212}Bi – ^{212}Po events and the anti-coincidence signals in the plastic scintillator light-guide and active shield, we have obtained a background counting rate of 0.28 counts/(yr \times keV \times kg) in the region of interest 2700 – 2900 keV.

We have tried to estimate the main sources of the detector background on the basis of the low background measurements and the Monte Carlo simulation: they are cosmogenic activation (most probably ^{110m}Ag), contamination of the $^{116}\text{CdWO}_4$ crystals by ^{228}Th (^{232}Th family), contribution of the 2615 keV γ peak of ^{208}Tl from details of the set-up. We are going to simulate all possible components of background; check radioactive contamination of PMTs, quartz, cables, copper (with aim to change the most contaminated elements); recrystallize the crystals to reduce the concentration of thorium.

The low background measurements to search for double β decay of ^{116}Cd with the help of the enriched cadmium tungstate crystal scintillators are in progress. The decrease of thorium con-

centration in $^{116}\text{CdWO}_4$ crystal scintillators, the decay of cosmogenic nuclides, the improvement of the pulse-shape analysis could further decrease the background to the level of $\sim 0.01 - 0.1$ counts/(yr \times keV \times kg), and therefore, improve sensitivity of the experiment up to $T_{1/2} \sim (0.5 - 1.5) \times 10^{24}$ yr over 5 years of measurements. It corresponds, taking into account the recent calculations of matrix elements [4, 5, 6], to the effective neutrino mass $\langle m_\nu \rangle \approx 0.4 - 1.4$ eV.

Further progress in the experiment to search for the double beta decay of ^{116}Cd can be advanced by applying a massive array of $^{116}\text{CdWO}_4$ crystals with improved energy resolution and good particle discrimination ability.

7. Acknowledgements

The research was supported in part by the Gran Sasso Center for Astroparticle Physics (L'Aquila, Italy). The group from the Institute for Nuclear Research (Kyiv, Ukraine) was supported in part through the Project "Kosmomikrofizyka-2" (Astroparticle Physics) of the National Academy of Sciences of Ukraine. Authors are very grateful to Prof. B.V. Grinyov and Dr. P.N. Zhmurin from the Institute for Scintillation Materials (Kharkiv, Ukraine) for kindly provided sample of LS-221 liquid scintillator. We would like to thank Dr. C. Salvo for his kind help in preparing equipment for the crystals annealing. It is a pleasure to gratitude the staff of the Chemistry Service of the Gran Sasso laboratory for their warm hospitality and valuable support.

References

- [1] Yu.G. Zdesenko, Rev. Mod. Phys. 74 (2002) 663;
S.R. Elliot, P. Vogel, Ann. Rev. Nucl. Part. Sci. 52 (2002) 115;
J.D. Vergados, Phys. Rept. 361 (2002) 1;
S.R. Elliot, J. Engel, J. Phys. G 30 (2004) R183;
F.T. Avignone III, G.S. King, Yu.G. Zdesenko, New J. Phys. 7 (2005) 6;
H. Ejiri, J. Phys. Soc. Japan 74 (2005) 2101;
H.V. Klapdor-Kleingrothaus, Int. J. Mod. Phys. E 17 (2008) 505;
F.T. Avignone III, S.R. Elliott, J. Engel, Rev. Mod. Phys. 80 (2008) 481;
A.S. Barabash, Phys. At. Nucl. 73 (2010) 162.
- [2] G. Audi, A.H. Wapstra, C. Thibault, Nucl. Phys. A 729 (2003) 337.
- [3] M. Berglund and M.E. Wieser, Pure Appl. Chem. 83 (2011) 397.
- [4] M. Kortelainen and J. Suhonen, Phys. Rev. C 76 (2007) 024315.
- [5] F. Šimkovic et al., Phys. Rev. C 77 (2008) 045503.
- [6] F. Iachello and J. Barea, Proc. XIV Int. Workshop on "Neutrino Telescopes", Venice, Italy, March 2011, in press.
- [7] F.A. Danevich et al., Phys. Rev. C 68 (2003) 035501.
- [8] F.A. Danevich et al., Z. Phys. A 355 (1996) 433.
- [9] P. Belli et al., Eur. Phys. J. A 36 (2008) 167.
- [10] P. Belli et al., Nucl. Instr. Meth. A 615 (2010) 301.

- [11] P. Belli et al., Proc. Int. Conf. NPAE–2010, 7–12.06.2010, Kyiv, Ukraine – Kyiv, 2011, p. 428; P. Belli et al., AIP Conf. Proc. 1304 (2010) 354.
- [12] F.A. Danevich et al., Phys. At. Nucl. 59 (1996) 1.
- [13] P. Belli et al., Phys. Rev. C 76 (2007) 064603.
- [14] F.A. Danevich et al., Phys. Rev. C 67 (2003) 014310.
- [15] A. Piepke et al., Nucl. Phys. A 577 (1994) 493.
- [16] G.P. Kovtun et al., Functional Materials 18 (2011) 121.
- [17] A.A. Pavlyuk, Ya.V. Vasiliev, L.Yu. Kharchenko, F.A. Kuznetsov, in: Proc. of the APSAM-92, Asia Pacific Society for Advanced Materials, Shanghai, 26-29 April 1992, Institute of Materials Research, Tohoku University, Sendai, Japan, 1993, p. 164.
- [18] Yu.A. Borovlev et al., J. Cryst. Growth 229 (2001) 305.
- [19] E.N. Galashov, V.A. Gusev, V.N. Shlegel, Ya.V. Vasiliev, Crystallogr. Rep. 54 (2009) 689.
- [20] M.E. Wieser and T.B. Coplen, Pure Appl. Chem. 83 (2011) 359.
- [21] L. Bardelli et al., Nucl. Instr. Meth. A 569 (2006) 743.
- [22] S. Agostinelli et al., Nucl. Instr. Meth. A 506 (2003) 250;
J. Allison et al., IEEE Trans. Nucl. Sci. 53 (2006) 270.
- [23] E. Gatti, F. De Martini, Nuclear Electronics 2, IAEA, Vienna, 1962, p. 265.
- [24] T. Fazzini et al., Nucl. Instr. Meth. A 410 (1998) 213.
- [25] F.A. Danevich et al., Phys. Lett. B 344 (1995) 72.
- [26] F.A. Danevich et al., Nucl. Phys. A 694 (2001) 375.
- [27] R.B. Firestone et al., *Table of Isotopes*, 8-th ed., John Wiley, New York, 1996 and CD update, 1998.
- [28] A.S. Barabash, Phys. Rev. C 81 (2010) 035501.
- [29] P. Belli et al., Nucl. Instr. Meth. A 626&627 (2011) 31.
- [30] F.A. Danevich et al., Nucl. Instr. Meth. A 631 (2011) 44.
- [31] G. Bellini et al., Eur. Phys. J. C 19 (2001) 43.
- [32] W.R. Nelson et al., SLAC-Report-265, Stanford, 1985.
- [33] O.A. Ponkratenko et al., Phys. At. Nucl. 1282 (2000) 63;
V.I. Tretyak, to be published.
- [34] R.N. Mohapatra et al., Phys. Lett. B 491 (2000) 143.